Conversion of hydrocarbon fuel in a thermal protection reactors of hypersonic aircraft

A. L. Kuranov, A. V. Korabelnikov* and A. M. Mikhaylov**
* Hypersonic Systems Research Enterprise of Leninetz HC
212 Moskovski prospekt Sankt-Peterburg Russia

Abstract
Thermal protection of heat-stressed surfaces of a high-speed vehicle flying in dense layers of atmosphere is one of the topical issues. Not of a less importance is also the problem of hydrocarbon fuel combustion in a supersonic air flow. In our concept under development it is supposed that in the most high-stressed parts of airframe and engine catalytic thermochemical reactors will be installed, wherein highly endothermic processes of steam conversion of hydrocarbon fuel take place. Simultaneously with heat absorption hydrogen generation will occur in the reactors. This paper presents the results of a study of conversion of hydrocarbon fuel in a slit reactor.

1. Introduction

Endothermic reactions as a method of cooling are considered by many researchers due to the necessity of removal and recovery of large heat fluxes. The use of different types of hydrocarbons as reagents allows, except removal of heat by the endothermic effect of the reaction, to obtain a hydrogen-containing fuel with better energy characteristics. The use of hydrocarbon fuel conversion for cooling heat-stressed areas of high-speed vehicles and organization of their burning in supersonic air flow have been considered by the experts from the sixties of the last century. It is well known, that the major drawback of hydrocarbon fuels resides in considerable (td ~ 10 ms), as compared to hydrogen (τd ~ 0.1 mc), times of ignition delay which leads to the necessity of long combustion chamber. However, mixing hydrogen produced in TCR with basic mass of kerosene results in decrease of ignition time for flammable mixture [1]. Thus, the considered concept solves both designated tasks.

2. Experimentation

Based on the application, it was decided to use flat TCR of 571 mm length, 60 mm width and 4 mm thick as a model of thermal protection element which brings it closer to the actual required shape. The particular properties of the selected heat source (ЭДП-109М; electric-arc plasmatron) necessitate thermal protection cover over the central channel, through which nitrogenous plasma jet, obtained in plasmotron, passes. The walls forming the channel are protectable. Geometrically, it was decided to make the central channel of a flat shape as well of a width exceeding the height significantly. Such a design provided an opportunity not to protect side walls, sufficiently distant from the core of the flow. Besides, as a result of the flow flattening, in the vicinity of the central vertical section, in the two-dimensional channel heat exchange is intensified. At the entrance to the TCR a mixer with tangential component in-feed was placed for ensuring mixing and their distribution between the upper and lower channels.
Framework of a model reactor is made of the XH78T alloy with onset scaling temperature in air making 1150 ºC and the maximum recommended operating temperature for a long period (up to 10 000 hours) corresponds to 1 100 º C. This alloy is used for the manufacture of flame tubes of high-temperature combustion chambers of turbojet engines operating at 1000 – 1 100 ºC. Another very important advantage of this alloy is the composition of its components which is very close to that of nichrome X20H80 previously used as catalytic coatings. This allows, after special treatment of the reactor internal surfaces, carrying out steam conversion of hydrocarbons directly on its wall.
To increase the degree of conversion of hydrocarbon fuels, special wireframe catalysts have been made. Such a catalyst is a compressed nichrome wire etched to increase specific surface area and activated in an oxygen atmosphere in a muffle furnace. A more detailed description of the experimental reactor can be seen in [2] or [3].
Experimentation was designed to determine modes of TCR of thermal protection with the maximum degree of conversion subject to the removal of significant heat flows. Apart from that, applicability of the selected material for TCR framework has been checked and operation of the new catalysts has been analyzed.

The input parameters of the experiment were: the flow of steam, methane flow, nitrogen flow in the plasmatron, the temperature of the mixture of water vapor and methane in the reactor inlet, plasmatron power. The main output parameters directly measured were: temperature of the cooled wall measured at six points and chemical composition of the mixture taken up in the sampling points. Based upon measured values of the input and output parameters it is possible to obtain heat flow rate, mixture flow rate, and conversion degree of methane.

2.2 Experimental results

A total of 4 sustained experiments have been carried out during which 11 steady-state regimes were investigated. The first experiment was carried out without wireframe catalyst in TCR. One steady-state mode was studied. Ratio of steam to methane consumption was taken in excess of stoichiometric one (H_2O / CH_4 ~2:1). Parameter values of steady-state regimes are presented in Table 1.

Table 1: Stationary mode of the 1st experiment

Mode N_0	Steam Consump-tion [g/s]	Methane consump -tion [g/s]	Plasma-tron power [κW]	Point 1 65 mm from beginning of reactor (BOR)	Point 2 153 mm from BOR	Point 3 247 mm from BOR	Point 4 332 mm from BOR	Point 5 431 mm from BOR	Point 6 501 mm from BOR
				Wall temperature [°C]					
				Conversion degree					
1.1	0.27	0.13	25.1	938 No data available	1028 0.11	1052 No data available	1041 0.27	1013 No data available	955 0.43

Due to the fact that plasmotron power was rather insufficient (14 kW) under significant consumption of the components (GH_2O = 0.27g/s; GCH_4 0.13g/s) temperature of the walls remained low leading to a low-level conversion degree without catalysts (0.43). The second and subsequent experiments were carried out with wireframe catalysts in TCR.

The 2nd experiment resulted in successful accomplishment of three (3) stationary modes. The component ratio at the reactor inlet was maintained at GH_2O/GCH_4 = 2:1. The 1st was a straight-through, with a significant subcooled wall (T_w < 650 ºC). Because the wall temperatures are below the ones at which the conversion rate of the steam is considerable, it can be said that this mode does not provide steam conversion. During 2nd mode the plasmotron power has been raised to 3.5 kW. The wall temperature has reached the value of 1000 ºC. Comparing this mode with one of the 1st experiment, it can be said that it is possible to constrain temperature at the same level under identical consumption and plasmotron power above 1.6 times. This points to significant increase in the rate of reaction - thanks to the catalyst. In the 3rd mode, plasmotron power was further raised to 49.8 kW, and besides, consumption of methane and water vapor has been raised too. Furthermore, the walls temperature has reached 1280 ºC. Table 2 shows the values of the parameters in the stationary mode.

Table 2: Stationary modes of the 2nd experiment

Mode N0	Water Steam consumption [g/s]	Methane consumption [g/s]	Plasmotron power [kW]	Point 1 65 mm from beginning of reactor (BOR)	Point 2 153 mm from BOR	Point 3 247 mm from BOR	Point 4 332 mm from BOR	Point 5 421 mm from BOR	Point 6 501 mm from BOR
				Wall temperature [oC]					
2.1	0.3	0.13	14.8	605	614	587	555	529	503
2.2	0.29	0.14	39.5	996	1049	1027	989	939	892
2.3	1	0.51	49.8	1206	1280	1272	1259	1242	1192

The 3rd experiment resulted in successful accomplishment of the two (2) stationary modes. The ratio of components was also maintained at the level GH_2O/GCH_4 = 2:1, while the 2nd mode differed from the 1st one in plasmotron power rise and insignificant buildup of methane consumption. Table 3 presents values of parameters in the stationary modes of the 3rd experiment.

Table 3: Stationary modes of the 3rd experiment

Mode N0	Water steam consumption [g/s]	Methane consumption [g/s]	Plasmotron power [kW]	Point 1 65 mm from beginning of reactor (BOR)	Point 2 153 mm from BOR	Point 3 247 mm from BOR	Point 4 332 mm from BOR	Point 5 421 mm from BOR	Point 6 501 mm from BOR
				Wall temperature [oC]					
3.1	0.26	0.12	16.3	717	756	760	749	739	710
3.2	0.26	0.13	29.9	1047	1100	1081	1065	1047	1007

During 4th experiment 5 stationary modes have been successfully accomplished. In the course of the first one the consumption was maintained at GH_2O/GCH_4 = 2:1 and during the second - GH_2O/GCH_4 = 4:3 – close to stoichiometric ratio. Further on three modes were investigated with the ratio GH_2O/GCH_4 – 9:11, i.e. with a significant deviation from stoichiometry in the area of excess methane. During the experiment the analysis of the chemical composition has been carried out (Fig.1). Concentrations of methane (CH_4) and the major products of the reaction – hydrogen (H_2) and carbonic oxide (CO) for each steady state have been subsequently determined lengthways of the reactor.

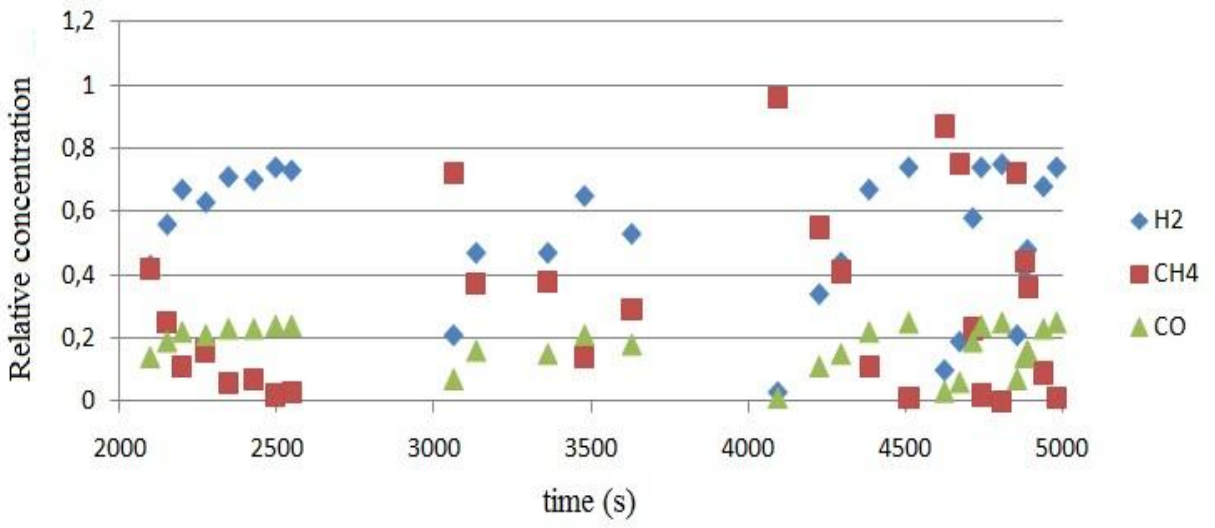

Figure 1: Relative gas concentration measuring

Table 4 presents the values of major parameters corresponding to the stationary modes of the 4th experiment. As can be seen, the modes were investigated with high plasmotron power and increased consumption where high temperature values have been obtained. It is also worth noting the high degree of conversion in all modes.

Table 4: Stationary modes of the 4th experiment

Mode N_0	Water Steam consumption [g/s]	Methane consumption [g/s]	Plasmotron power [kW]	Point 1 65 mm from beginning of reactor (BOR)	Point 2 153 mm from BOR	Point 3 247 mm from BOR	Point 4 332 mm from BOR	Point 5 421 mm from BOR	Point 6 501 mm from BOR
				Wall temperature [^{o}C] Conversion degree					
4.1	0.26	0.13	26.1	945 No data available	1015 0.58	1010 0.75	997 0.89	984 0.94	946 0.98
4.2	0.44	0.33	30.1	947 No data available	1038 0.28	1045 0.62	1035 No data available	1019 0.71	976 0.86
4.3	0.44	0.54	30	910 No data available	1015 0.04	1036 0.45	1030 0.59	1015 0.89	976 0.99
4.4	0.45	0.53	51	1146 No data available	1195 0.13	1163 0.25	1147 0.77	1112 0.98	1069 1
4.5	0.45	0.54	60.2	1266 No data available	1290 0.28	1246 0.56	1225 0.64	1193 0.91	1141 0.99

3. Mathematical model

The experimental data obtained are insufficient for a description of the heat-and-mass transfer processes under investigation since not all physical values could be measured in the experiments. To determine such values it is necessary to use the tools of mathematical modeling. Based on the data obtained in the course of the experiments, it is possible to create a model that describes the relationship of the target values under conducted experiments.

First of all, it is necessary to determine the distribution of the value of specific heat flow issuing from the nitrogen plasma and absorbing in TCR. It is the principal criterion for the applicability of steam conversion in the elements of the active thermal protection.

Next, one needs to evaluate the relative efficiency of the TCR (with catalytic filling) operation in the implemented modes. For experiments in which there was no data on gas composition, it is necessary to calculate the distribution of the reacting mixture. To determine all these parameters, a model was developed which consists of two parts.

The first part of the central channel model describes the interaction of the nitrogen plasma jet and the TCR's metal wall with the known measured temperature; distribution of specific heat flow is determined here. The 2nd part of the channel model describes the processes that occur directly inside the TCR, namely, heating and chemical transformations of the component flow. The rate and composition of the reacting mixture are determined from the 2nd part of the model, the calculation is based on the determined distribution of specific heat flow. Mathematical calculations were carried out in the environment of finite-difference simulation – Comsol 4.3a. The module "Conjugate Heat Transfer" describing the conductive and convective heat transfer in media and solids moving according to laminar laws was used in the 1st part of the experimental model. In the 2nd part of the model the modules "Darcy's Low", "Heat Transfer in Fluids", and "Transport of Concentrated Species" have been used. These modules together describe hear transfer and thermo-chemical processes for multicomponent mixture flowing in a porous medium.

3.2 The model of the central channel

Geometrically, the model of the central channel is a channel ABCD 571mm long and 20mm wide with walls having a thickness 4mm (Fig.2). The heated in plasmotron nitrogen travels into the channel over the edge AB. While passing through the central channel, nitrogen heats the wall.

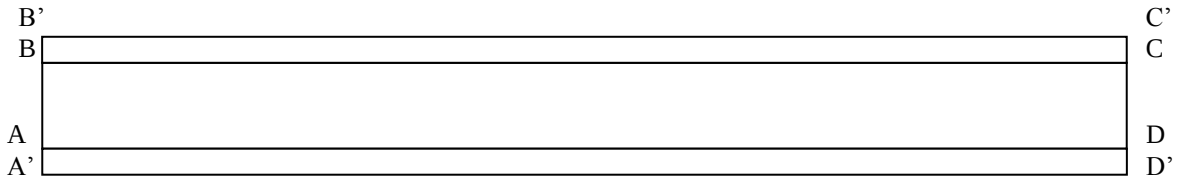

Figure 2: The geometrical representation of the central channel model

Flow and heat transfer in the central channel ABCD are described by a set of equations below:

$$\begin{cases} \rho\frac{\partial\vec{u}}{\partial t}+\rho(\vec{u}\times\nabla)\vec{u}=\nabla\times\left(-\rho\vec{I}+\mu(\nabla\vec{u}+(\nabla\vec{u})^{T})\right)+\vec{F} \\ \rho\nabla\times\vec{u}=0 \\ \rho C_p\frac{\partial T}{\partial t}+\rho C_p\vec{u}\times\nabla T=\nabla\times(k\nabla T)+Q \end{cases},$$

ρ – density [kg/m^3]; $\vec{u}$ – velocity vector [m/s]; t – time [s]; $\vec{I}$ - identification matrix; μ – dynamic viscosity [Pa*s] ; $\vec{F}$ – baric gradient [Pa/m]; C_p- heat capacity at constant pressure [J/(K*kg)]; *k* – thermal conductivity [W/(m*K)]; Q – flow of heat [W].

Boundary conditions in BC and AD are as follows: $\vec{u}=0$.

Boundary conditions in AB determine nitrogen flow m[g/s]:

$$-d_{bc}\int_{\partial\Omega}\rho(\vec{u}\times\vec{n})dS=m$$

And concurrent heat flow q_0[W]:

$$-\vec{n}\times(-k\nabla T)=\left(-q_0(\vec{u}\times\vec{n})\frac{\int l}{\int|\vec{u}\times\vec{n}|}\right)+\rho(\Delta h_{in}-\Delta h_{\infty})\vec{u}\times\vec{n}$$

, where $\Delta h_{in}-\Delta h_{\infty}=\int_{T_{\infty}}^{T_{in}}C_p dT+\int_{P_{\infty}}^{PT_a}\frac{1}{\rho}\left(1+\frac{T}{\rho}\left(\frac{\partial\rho}{\partial T}\right)|_p\right)dp$.

Boundary conditions in CD determine free out flow of nitrogen into the medium with pressure p_0=100 kPa:

$$p=p_0$$
$$\left(\mu(\nabla\vec{u}+(\nabla\vec{u})^{T})-\frac{2}{3}\mu(\nabla\times\vec{u})\vec{I}\right)\times\vec{n}=0.$$

Besides, the heat output in CD is determined only as nitrogen heat:

$$-\vec{n}\times(-k\nabla T)=0.$$

Heat transfer in the walls AA'D'D and BB'C'C is described by heat-transfer equation:

$$\rho C_p \frac{\partial T}{\partial t} + \rho C_p \vec{u} \times \nabla T = \nabla \times (k \nabla T) + Q.$$

Boundary conditions for the walls are: thermal isolation of the walls AA', BB', CC' and DD': $-\vec{n} \times (-k\nabla T) = 0$, and for the A'D' and B'C' – the temperature corresponding to the wall temperature at the test of free-scale model, determined by interpolation of the experimental data: *T = T0(t,x)*

3.3 The model of TCR channel

In the two-dimensional approximation TCR is a rectangular channel (Fig.3) in which from cross-section EF to the cross-section GH a reactive mixture flows. The channel is filled with porous catalyst. The mix is changing with depleting of the initial components. If at the input it consists of methane and water steam, the main components of the output are carbon monoxide and hydrogen. FG wall is heat-insulated, and through the wall EH, the temperature of which corresponds to the wall temperature of the full-scale model of the experiment, passes heat flow, determined by the 1st part of the mathematical model of the experiment.

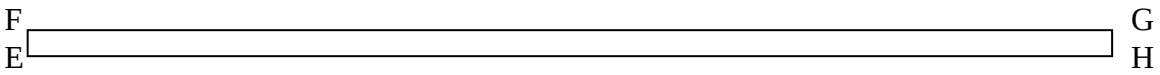

Figure 3: Geometrical representation of the TCR model

The processes occurring in the reactor are described by the following system of equations:

$$\begin{cases} \frac{\partial}{\partial t}(\rho \varepsilon_p) + \nabla(\rho \vec{u}) = Q_m \\ \rho C_p \frac{\partial T}{\partial t} + \rho C_p \vec{u} \times \nabla T = \nabla \times (k \nabla T) + Q, \\ \rho \frac{\partial \omega_i}{\partial t} + \nabla \times \vec{J_i} + \rho(\vec{u} \times \nabla)\omega_i = R_i \end{cases}$$

Where: $\vec{u} = -\frac{K}{\mu}\nabla p$; $\vec{J_i} = -(\rho D_i^m \nabla \omega_i + \rho \omega_i D_i^m \frac{\nabla M_n}{M_n} + D_i^T \frac{\nabla T}{t})$; $\vec{N_i} = \vec{J_i} + \rho \vec{u} \omega_i$; $D_i^m = \frac{1-\omega_i}{\sum_{k \neq i} \frac{x_k}{D_{ik}}}$;

$$M_n = (\sum_i \frac{\omega_i}{M_i})^{-1};$$

t – time [s]; ρ – density [kg/m^3]; ε_p– porosity index; $\vec{u}$ – velocity vector [m/s]; Q_m – flow of heat from reaction [W]; C_p – heat capacity at constant pressure [J/(K*kg)]; *T* – temperature [K]; K – hydraulic conductivity [m/s]; *k* – thermal conduction [W/(m*K)]; ω_i–mass fraction of component i; $\vec{J_i}$ – source power of i component [kg/s]; R_i– mass velocity of reaction [kg/(m^3*s)]; D_{ik} – coefficient of mutual diffusion I and k components [m^2/s]; D_i^T - thermal diffusion coefficient [kg/(m*s)]; x_k – volume ratio of k component; M_i– molar mass of i component [g/mole].
The 1st equation in the system is the equation of Darcy's law, the 2nd one – heat-transfer equation, and the 3rd – law of dynamics for every mixture component
The boundary conditions on EF are described by the system:

$$\begin{cases} -\vec{n} \times \rho \vec{u} = 0 \\ T = T_w \\ -\vec{n} \times \vec{N_1} = 0 \end{cases}$$

Where Tw – wall temperature.
The boundary conditions on EF are described by the system:

$$\begin{cases} -\vec{n} \times \rho \vec{u} = \mathrm{N_0} \\ T = T\varepsilon x \\ \omega_i = \omega_{0i} \end{cases},$$

where Tim –temperature of the input mixture;
N_0 – nitrogen consumption; ω_{0j} – initial mass content of components.
The boundary conditions on FG are described by the system:

$$\begin{cases} -\vec{n} \times \rho\vec{u} = 0 \\ -\vec{n} \times (-k\nabla T) = 0 \\ -\vec{n} \times \overrightarrow{N_i} = 0 \end{cases}$$

The boundary conditions on GH are described by the system:

$$\begin{cases} p = p_0 \\ -\vec{n} \times (-k\nabla T) = 0, \\ -\vec{n} \times \rho D_i^m \nabla\omega = 0 \end{cases}$$

where p_0 –output pressure.
For performing calculations, the net was used with variable cell sizes dictated by the intensity of parametric variation. The initial condition for the calculation was chosen to be the state of the full-scale model before plasmotron startup. The calculation of each step was carried out using MUMPS technique (MUltifrontal Massively Parallel sparse direct Solver) with non-linear Newtonian steps. Time steps were carried out by the method of reverse differentiation formulas.
For calculation purposes, experimental findings I, II, and III have been used, namely, the readings from sensors of wall temperature, current and voltage sensors of plasmotron, temperature and cooling water consumption, nitrogen and methane consumption, readings of measuring complex for water steam, mix temperature at the TCR inlet. Temporal functional relationship was determined for all parameters by method of spline interpolation of sensor readings. Distribution of temperatures alongside the reactor on the basis of the wall temperature sensor readings was also determined.

3.4 Calculation results

As a result of calculations, temporal dependencies of distribution for temperature, vector field of the heat flow, mix composition, vector field of the velocity have been obtained.

Table 5: Absorbable heat flux

Time	**Qc1 kW/m^2**	**Qc2 kW/m^2**	**Qc3 kW/m^2**	**Qc4 kW/m^2**	**Qc5 kW/m^2**	**Qc6 kW/m^2**
The model of the central channel						
2700	18.2	9.4	6.9	6.4	6.1	6.5
3800	30	17	11	10.8	10.9	11.5
4300	31.4	17.2	11.4	11	10.9	11.2
4750	53.6	38.7	30.2	27.7	27.1	28.4
4825	69.9	40.6	29.3	27.3	26.5	25.5
TCR model						
2700	20.1	10.7	7.8	7.2	6.6	6.8
3800	32.4	19.2	12.5	12.2	12.2	12.7
4300	33.9	19.5	13.2	12.6	12.4	12.7
4750	58	42.1	32.6	29.8	28.8	29.9
4825	74.7	44.3	31.9	29.5	28.3	27.1

As can be seen from the Table 5, the calculations on various models brought almost similar results. It is worth noting, that in the area of small values, heat flow magnitude obtained by the calculation from TXP model is most different from the one calculated by the model of the central channel. Under the test conditions, the magnitude of the

heat flux was determined by temperature of the wall heated by plasmotron. This relationship is shown in Figure 4. An important parameter is the specific heat absorption.
Dependence of the specific heat absorption on the specific heat flow are presented in Fig.5.

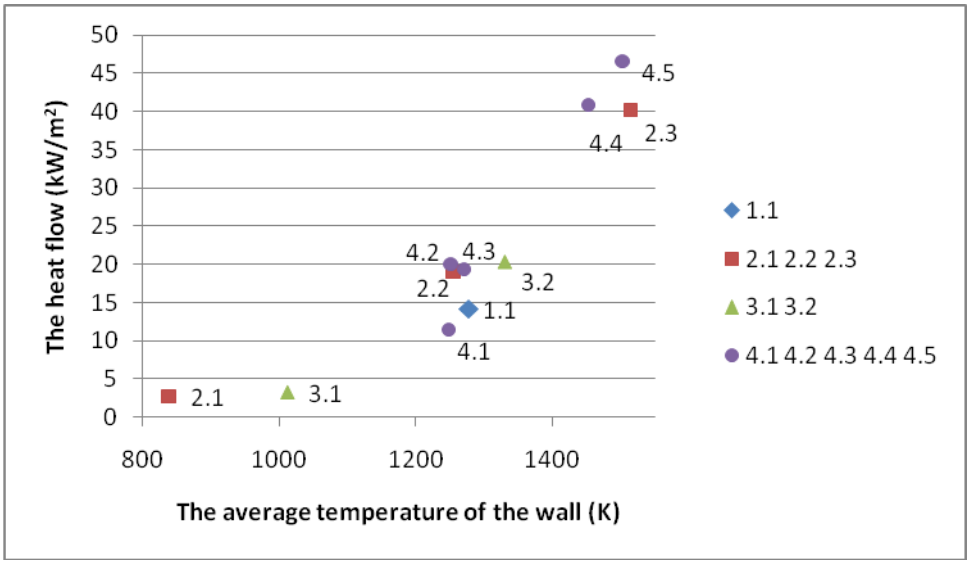

Figure 4: The dependence of the average heat flux on the average wall temperature

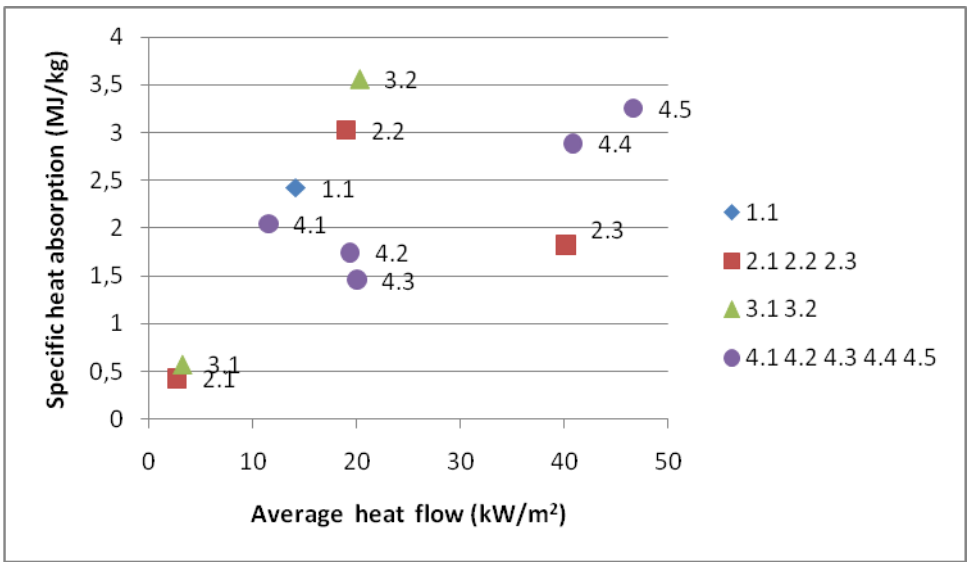

Figure 5: Dependence of specific heat absorption on the average heat flow

As can be seen, some experiments resulted in getting specific heat absorption values equal to 3 MJ/kg. However, in several experiments with a high degree of conversion, specific heat absorption was less than 2 MJ/kg. Since the theoretical maximum value of specific heat absorption for a mixture of methane and water with a stoichiometric component ratio makes ~ 8 – 10 MJ/kg, including chemical cooling capacity of 6 MJ/kg, it would be proper to say that the mixture absorbs only from 17% to 63% of the total cooling capacity in modes with a high degree of conversion directly from the cooled wall.
Table 6 compares experimental and theoretical values of the specific heat absorption. As can be seen, cooling capacity efficiency to cool the walls in different experiments varies greatly, though conversion degree remains high. This is due to the fact that during the preparation and mixing the components absorb sufficient heat to ensure a high degree of conversion, and the heat from the wall, though contributing significantly to the heat balance, does not affect the conversion.

Table 6: Specific heat absorption and efficiency of cooling capacity

Mode	Specific heat absorption experiment MJ/kg	Specific heat absorption teoretical MJ/kg	Efficiency of Cooling capacity inside TCR %
1.1	2.42	5.53	44
2.1	0.42	5.14	8
2.2	3.02	5.54	55
2.3	1.82	5.74	32
3.1	0.57	5.37	11
3.2	3.56	5.67	63
4.1	2.04	5.96	34
4.2	1.74	7.39	24
4.3	1.45	8.81	17
4.4	2.88	9.01	32
4.5	3.25	9.19	35

4. Conclusion

The selected material was under treatment for more than 100 minutes subjected to high temperatures exceeding 1000° C. Subsequently, neither mechanical changes were spotted on it, no traces of scale formation observed. The applied catalyst allowed not only markedly increase conversion degree but also improve thermal protection. In the experiments carried out with a catalyst fixed, high values of conversion degree for methane were obtained. A wide range of experimental parameters for assessing the performance of the reactor as part of a thermal protection in the modes with low heat fluxes and high degrees of conversion has been covered in this paper.

References

[1] Kuranov A.L., Korabelnikov A.V. and Mikhailov A.M. 2012. Thermal protection and hydrogen production on board of the hypersonic vehicle 18th AIAA/3AF International Space Planes and Hypersonic Systems and Technologies Conference Tours France.

[2] Kuranov A.L., Korabelnikov A.V. and Mikhailov A.M. 2012. Experimental study of steam reforming of methane in the thermochemical reactor. International Symposium on "Thermochemical processes in plasma aerodynamics" St. Petersburg Russia.

[3] Kuranov A.L., Korabelnikov A.V. and Mikhailov A.M. 2012. Application of steam conversion of hydrocarbonic fuel in hypersonic aircraft power installations. International Conference on the Methods of aerophysical research(ICMAR) Kazan Russia.